Journal of the Korean Chemical Society
2023, *Vol. 67, No. 1*
Printed in the Republic of Korea
https://doi.org/10.5012/jkcs.2023.67.1.64

Note

Fluorescence Correlation Spectroscopy of Macromolecules Using Maximum Entropy

Hahkjoon Kim
Department of Chemistry, College of Natural Science and Technology, Duksung Women's University, Seoul 01369, Korea.
E-mail: khj730516@duksung.ac.kr
(Received November 28, 2022; Accepted December 15, 2022)

Key words: Quantum dot, Lipid vesicle, Maximum entropy, Fluorescence correlation spectroscopy (FCS)

Semiconductor quantum dots (QDs) have attracted wide interest in chemical sensing applications such as bioimaging because of their unique size-dependent properties and robust luminescence.[1–3] To dissolve semiconductor QDs in water, their surfaces are coated with hydrophilic groups. Various ligands are then bound to the surface of the QDs in order to bind them to specific compounds. These surface treatments increase the nonspecific binding of QDs and can cause their aggregation.[4–6] Fluorescence correlation spectroscopy (FCS) is a sensitive analytical method that measures the concentration and diffusion coefficient of fluorescent molecules by analyzing the fluorescence intensity fluctuation (based on photon count correlations) that occurs as the molecules pass through the laser focus.[7–10]

FCS has a wide range of applications, including in the analysis of molecular diffusion, structural changes in macromolecules, aggregation, chemical reactions, and intersystem crossing of fluorescent molecules.[11–16] When the fluorescence intensities at times t and $t+\tau$ are $F(t)$ and $F(t+\tau)$, respectively, the autocorrelation function $G(\tau)$ is given by[17]

$$G(\tau)=\frac{\langle F(t)\rangle\langle F(t+\tau)\rangle}{\langle F\rangle^2}=1+\frac{\langle \delta F(0)\delta F(\tau)\rangle}{\langle F\rangle^2}, \qquad (1)$$

where $\delta F(t)=<F>-F(t)$. Assuming the focal point of the laser light formed by the objective lens is Gaussian with radius r and height s, the autocorrelation function arising from the diffusion of a single component is given by[18–19]

$$G(\tau)=\frac{1}{N}\left(1+\frac{\tau}{\tau_D}\right)^{-1}\left(1+\left(\frac{s}{r}\right)^2\frac{\tau}{\tau_D}\right)^{-\frac{1}{2}}=\frac{1}{N}D(\tau), \qquad (2)$$

where N is the average number of fluorescent molecules and τ_D is the average retention time of the molecules in the focal volume. The diffusion coefficient of the fluorescent molecule is given by

$$\boldsymbol{D}=\frac{r^2}{4\tau_D}=\frac{kT}{6\pi\eta\alpha}, \qquad (3)$$

where k is Boltzmann's constant, T is the absolute temperature, η is the viscosity of the solution, and α is the hydrodynamic radius of the diffusing species.

When the radius of the laser focus is fixed, the diffusion coefficient (D) and retention time (τ) of the two diffusers are given by

$$D_1\tau_1=D_2\tau_2, \qquad (4)$$

where subscripts 1 and 2 denote the two diffusing species. The radius of species 2 is expressed as follows:

$$a_2=\frac{\pi_2 kT}{6\pi\eta D_2\tau_2}. \qquad (5)$$

The autocorrelation function resulting from the multicomponent diffusion is given by

$$G(\tau)=\sum_{i=1}^{n}b_i\left(\frac{1}{1+\frac{\tau}{\tau_{Di}}}\right)\left(\frac{1}{1+\left(\frac{s}{r}\right)^2\frac{\tau}{\tau_{Di}}}\right)^{1/2}, \qquad (6)$$

where b_i and τ_{Di} are the amplitude and diffusion time, respectively, of the ith diffusion species. The least-squares fitting algorithm is a commonly used method to fit the fluorescence intensity fluctuations arising from single-component fluorescent molecules. However, data fitting using Eq. (4) is challenging when the system is highly heterogeneous. Maiti *et al*. developed a maximum entropy fluorescence correlation spectroscopy (MEMFCS) algorithm as a method to obtain diffusion constants of heterogeneous systems by fitting FCS curves.[20] MEMFCS has been

widely used to obtain the size distribution of heterogeneous macromolecules.[21–22] The principle of maximum entropy states that the probability distribution that best represents the current state of a system is the distribution with the largest entropy, in the context of precisely specified prior data. The autocorrelation function for fluorescence fluctuations generated from fluorescent materials with diffusion times between $\tau_D(1)$ and $\tau_D(2)$ is as follows:[20]

$$G(\tau) = \int_{\tau_D(1)}^{\tau_D(2)} a(\tau_D)\left(\frac{1}{1+\frac{\tau}{\tau_{Di}}}\right)\left(\frac{1}{1+\left(\frac{s}{r}\right)^2\frac{\tau}{\tau_{Di}}}\right)^{1/2} d\tau_D . \quad (7)$$

Here, $a(\tau_D)$ is the amplitude of the component whose diffusion coefficient is τ_D, and satisfies the following equation:

$$G(0) = \int a(\tau_D)d\tau_D . \quad (8)$$

where, $G(0) = 1/N$ in Eq. (2). A single-component data fitting was performed on TAMRA using SymPhoTime64 data analysis software. For the FCS of 200 nm lipid vesicles and QD605 with a heterogeneous distribution, the MEMFCS fitting program was used.

In this study, we investigated the size distribution of fluorescent lipid vesicles and QD605 in solution by using MEMFCS. We then calculated the number of QD605 QDs per aggregate based on the size distribution derived from MEMFCS.

Fig. 1 shows the FCS curve of the 20 nM TMR solution and its fit using Eq. (2). Based on data fitting, the diffusion time is 125 μs and N = 11.5. Because the initial concentration of TAMRA was 20 nM and the focal volume was ~1 fL, the radius of the laser focus was calculated to be ~360 nm using the known diffusion coefficient of TAMRA (2.6×10^{-10} m^2/s).

Fig. 2 shows the fit of the FCS curve for the 200 nm DiI POPC along with the size distribution derived from the MEMFCS algorithm. The fit shown in *Fig.* 2(a) is obtained using the MEMFCS algorithm with the number of diffusing species set at 100. *Fig*. 2(b) shows the distribution of the hydrodynamic radius of the DiI POPC derived from MEMFCS fitting. These results show that the radii of the lipid vesicles have a narrow distribution, with peaks centered at approximately 10 nm and 110 nm. Small unilamellar vesicles are made by passing giant multilamellar vesicles through a membrane with a pore size of 200 nm several

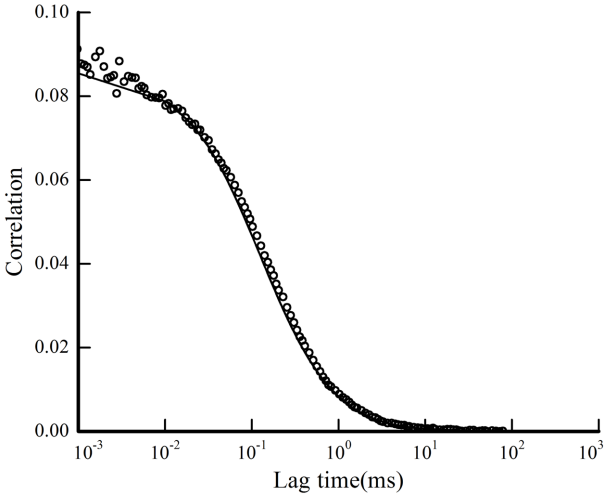

***Figure* 1.** FCS curve (open circle) and fit (solid line) of 20 nM TMR solution using Eq. (3).

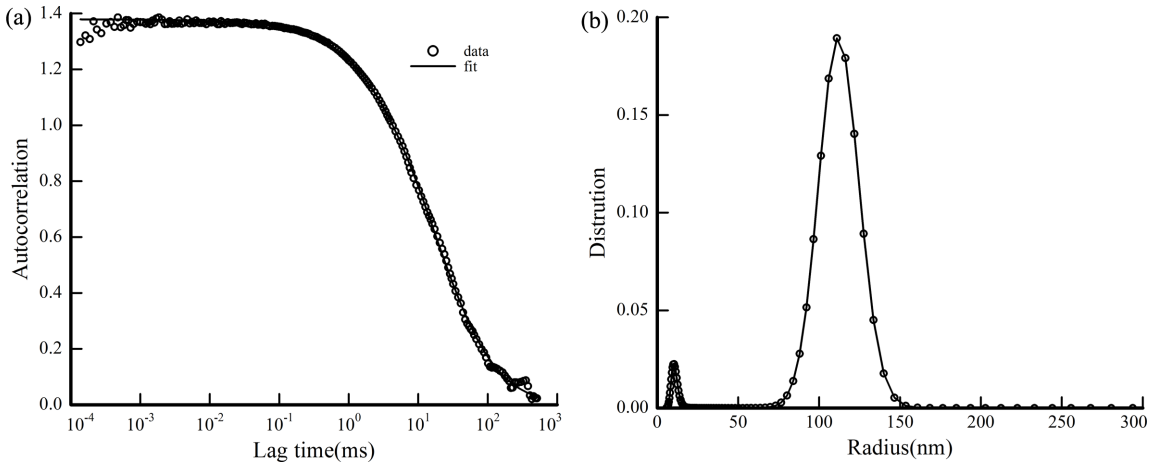

***Figure* 2.** (a) FCS curve (open circle) and fit (solid line) of DiI POPC using MEMFCS (b) Size distribution of DiI POPC obtained from MEMFCS.

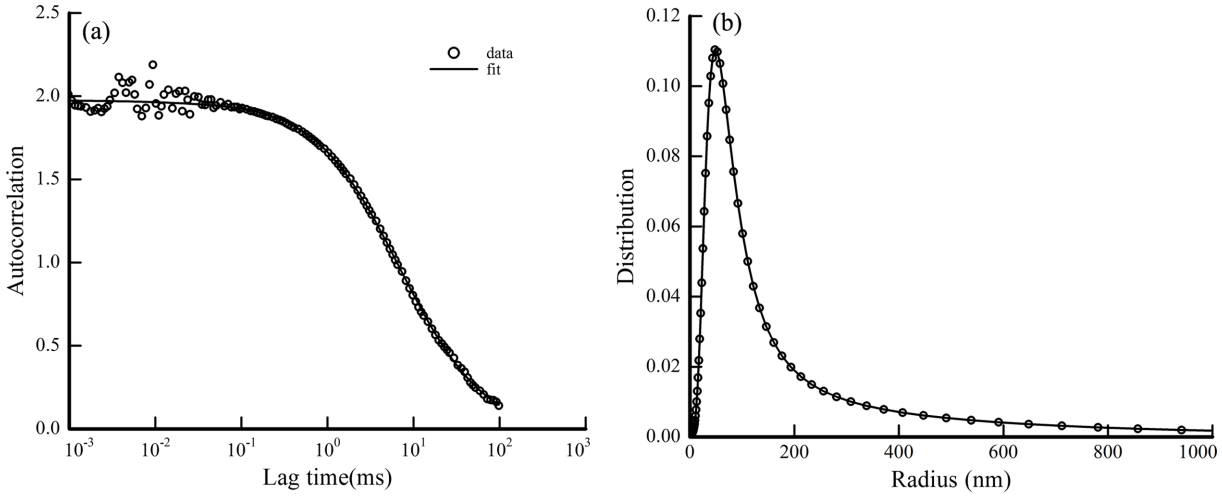

***Figure* 3.** (a) FCS curve (open circle) and fit (solid line) of QD605 using MEMFCS (b) Size distribution of DiI POPC obtained from MEMFCS.

times using a mini extruder. The production of lipid vesicles with a 110 nm hydrodynamic radius is expected when using an extrusion membrane with a pore size of 200 nm. However, the presence of small lipid vesicles with radii less than 10 nm, which cannot be measured by conventional FCS analysis, is an interesting and unexpected result. These small lipid vesicles are formed during the hydration of dried lipids. Because the size of the vesicles does not change, even when they continuously pass through the membrane pores, they appear to exist in their original state.

Fig. 3(a) shows the FCS curve and MEMFCS fit of QD605. The number of diffusion components used in the MEMFCS algorithm to fit the FCS profile of QD605 was 100. As shown in *Fig.* 3(b), the QD605 size distribution has a peak centered at ~70 nm followed by a long tail, resulting in an average radius of 170 nm. Unlike lipid vesicles, which do not aggregate, QD605 can form aggregates of variable sizes. The number of QDs per aggregate is determined using the radii of the aggregate and QD605. The radius (r) of a particle can be expressed as

$$r = \sqrt[3]{\frac{3M}{4\pi} \times \frac{1}{\rho}}, \tag{9}$$

where M is the molar mass, ρ is the density of the particle. Assuming that the aggregate density is constant during aggregation, $M \propto r^3$. Based on the average radius of biotinylated QD605 (~10 nm), the average number of QDs per aggregate is (167 nm/10 nm)^3 ≈ 4,600. Because the surface of QD605 is coated with biotin, aggregation easily occurs due to the sulfur, amine, and carboxyl groups present in biotin. However, the aggregation of QDs can be affected by variables such as the composition of the incubation buffer, including the ionic strength and protein type. Therefore, it is necessary to further study the effects of various environmental factors on the formation of QD aggregates.

In conclusion, we determined the size distribution of lipid vesicles using the MEMFCS fitting algorithm and confirmed that lipid vesicles of the expected size were produced. We were also able to measure small lipid vesicles that could not be detected using conventional FCS method. In addition, we analyzed the FCS profile of QDs using MEMFCS to obtain the size distribution and degree of aggregation. MEMFCS is a reliable method for studying the aggregation of QDs in solution because it enables an accurate size distribution analysis of QDs in solution.

EXPERIMENTAL

FCS experiments were performed using an inverted fluorescence microscope (IX-71, Olympus, Tokyo, Japan) equipped with a TIRF objective lens (alpha plan-apochromat, Zeiss, Oberkochen, Germany). The glass cover slip for placing the sample was coated with a POPC(1-palmitoyl-2-oleoyl-*sn*-glycero-3-phosphocholine, POPC, Avanti Polar Lipids, Alabaster, AL, USA) lipid bilayer having a size of about 100 nm after incubation for 1 hour and then wiped off. The sample on the cover slip was excited by pulsed laser light (510 nm, Picoquant, Berlin, Germany) passing through the objective lens, and fluorescence generated from the sample was collected by the same objective lens and sent out of the microscope. This fluorescence was

confocalized by a pinhole (75 μm, Thorlabs, Newton, NJ, USA) and sent to the GaAs PMT (H7421-50, Hamamatsu, Shizuoka, Japan). The time information of the fluorescence reaching the detector was recorded by a time correlated single photon counter (Timeharp 260 PICO, Picoquant, Berlin, Germany), which recorded the change in fluorescence intensity over time. Control of the entire equipment and data collection were performed through the Symphotime 64 program (Picoquant, Berlin, Germany). Fluorescent small unilamellar vesicles (SUVs) were prepared through the following process. First, POPC and 1,1'-Dioctadecyl-3,3,3',3'-Tetramethylindocarbocyanine Perchlorate (DiIC18, Avanti Polar Lipids, Alabaster, AL, USA) was dissolved in methylene chloride (Merck, Rahway, USA)/methanol (Merck, Rahway, USA) solution in a molar ratio of 1000 : 1. This solution was placed in a glass test tube, and the solvent was evaporated by a stream of nitrogen gas so that the POPC/DiI were uniformly coated on the wall of the glass test tube. To completely evaporate the solvent, this test tube was placed in a vacuum dessicator for 5 hours. The dried lipid mixture was vortexed with an phospate buffered saline (PBS, Merck, Rahway, USA) solution to obtain Giant multilamella vesicless (GMVs). The 100 nm SUVs were made by passing it through a mini extruder (Avanti Polar Lipids, Alabaster, AL, USA) equipped with a polycarbonate membrane filter with a pore size of 200 nm several times. The total concentration of POPC was 1 mg/mL. QD605 biotin conjugate used in this experiment was purchased from ThermoFischer (Waltham, USA) and dissolved in 10 mM $NaHCO_3$ (Merck, Rahway, USA).

Acknowledgments. This research was supported by Duksung Women's University Research Grants (3000005400).

REFERENCES

1. Chan, W. C. W.; Nie, S. *Science* **1998**, *281*, 2016.
2. Bruchez, M., Jr.; Moronne, M.; Gin, P.; Weiss, S.; Alivisatos, A. P. *Science* **1998**, *281*, 2013.
3. Jaiswal, J. K.; Mattoussi, H.; Mauro, J. M.; Simon, S. M. *Nat.Biotechnol.* **2003**, *21*, 47.
4. Mandal, S.; Gole, A.; Lala, N.; Gonnade, R.; Ganvir, V.; Sastry, M. *Langmuir* **2001**, *17*, 6262.
5. Starck, P.; Ducker, W. A. *Langmuir* **2009**, *25*, 2114.
6. Radhakrishnan, C.; Lo, M. K. F.; Knobler, C. M.; Garcia-Garibay, M. A.; Monbouquette, H. G. *Langmuir* **2011**, *27*, 2099.
7. Rigler, R.; Mets, U.; Widengren, J.; Kask, P. *Eur. Biophys. J.* **1993**, *22*, 169.
8. Schwille, P.; Haupts, U.; Maiti, S.; Webb, W. W. *Biophys. J.* **1999**, *77*, 2251.
9. Kannan, B.; Har, J. Y.; Liu, P.; Maruyama, I.; Ding, J. L.; Wohland, T. *Anal. Chem*. **2006**, *78*, 3444.
10. Varghese, L.; Sinha, R.; Irudayaraj, *J. Anal. Chim. Acta* **2008**, *625*, 103.
11. Magde, D.;. Elson, E. L.; Webb, W. W. *Biopolymers*, **1974**, *13*, 29.
12. Günther, J.-P.; Börsch, M.; Fischer, P. *Acc. Chem. Res*. **2018**, *51*, 1911.
13. Bonnet, G.; Krichevsky, O.; Libchaber, A. *Proc. Natl. Acad. Sci. U.S.A*. **1998**, *95*, 8602.
14. Magde, D.; Elson, E. L.; Webb, W. W. *Phys. Rev. Lett*. **1972**, *29*, 705.
15. Rauer, B.; Neumann, E.; Widengren, J.; Rigler, R. *Biophys. Chem*. **1996**, *58*, 3.
16. Lee, S.; Kim, H. *Bull. Korean Chem. Soc*. **2021**, *42*, 80.
17. Rigler, R.; Mets, U.; Widengren, J.; Kask, P. *Eur. Biophys. J.* **1993**, *22*, 169.
18. Aragon, S. R.; Pecora, R. *J. Chem. Phys*. **1976**, *64*, 1791.
19. Krichevsky, O.; Bonnet, G. *Rep. Prog. Phys*. **2002**, *65*, 251.
20. Sengupta, P.; Garai, K.; Balaji, J.; Periasamy, N.; Maiti, S. *Biophys J.* **2003**, *84*, 1977.
21. Chen, J.; Wang, C.; Irudayaraj, J. *J. Biomed. Opt*. **2009**, *14*, 040501.
22. Chen, J.; Nag, S.; Vidi, P.; Irudayaraj, J. *PLoS ONE* **2011**, *6*, e17991.